

See discussions, stats, and author profiles for this publication at: <https://www.researchgate.net/publication/356221590>

# Fault Diagnosis of Rotary Machines based on Vibration Signature and Machine Learning Algorithm

Article · October 2021

DOI: 10.21608/erjsh.2021.225704

CITATIONS

0

READS

113

3 authors, including:



**Mahmoud Mohamed Elsamanty**

Benha University

26 PUBLICATIONS 57 CITATIONS

[SEE PROFILE](#)



**A.A. Ibrahim**

Benha University

35 PUBLICATIONS 116 CITATIONS

[SEE PROFILE](#)

Some of the authors of this publication are also working on these related projects:



Condition monitoring of rotating machinery using adaptive wavelet analysis [View project](#)



Fault Diagnosis of Rotary Machines based on Vibration Signature [View project](#)



# Fault Diagnosis of Rotary Machines based on Vibration Signature and Machine Learning Algorithm

Mahmoud Mohammed Elsamanty<sup>a,c</sup>, Wael Saady Salman<sup>a,b</sup>, AbdElkader AbdElkareem Ibrahim<sup>a</sup>

<sup>a</sup> Faculty of Engineering at Shoubra, Benha University, Shoubra, Cairo, Egypt

<sup>b</sup> Fayoum University, Faculty of Engineering, Mechanical Department, Fayoum, Egypt

<sup>c</sup> Smart Engineering Systems Research Center (SESC), Nile University, Shaikh Zayed City, Giza, Egypt

**Abstract :** Fault diagnosis of rotating machines is one of the most considered maintenance methods for detecting faults early to save maintenance cost and time. In this work, an improvement technique is presented using back propagation neural network (BPNN) based vibration data to detect different faults in rotating machines such as unbalance, pulley misalignment, belt damage, and combined faults. The root means square (RMS) of vibration signals at different points was collected and employed as an input vector to the network. It was observed that the test and validation performance achieve the same pattern and the best validation was recorded at 0.33038 mean squared error (MSE). This training accuracy can identify combined pulley misalignment with unbalance, static unbalance on two shafts, dynamic unbalance, and combined belt damage with unbalance faults with identification accuracy of 95, 92, 88, and 80%, respectively. Static unbalance, pulley misalignment, and belt damage faults come in the second level of accuracy since they have the same accuracy of 75%. Furthermore, this network has a superior improvement in detecting combined faults in addition to other single variable faults.

**Keywords:** (Condition Monitoring, Rotating Machine, Machine Learning, Neural Network, Fault Diagnosis)

## 1. Introduction

Rotary machines in general configuration consist of three main parts; rolling or journal bearings (anti-friction or fluid bearings), rotor, and foundation. Since rotary machines commonly work in a harsh operating environment, this makes them more exposed to different types of faults and increases the difficulty of fault diagnosis. The failure in rotating machines leads to decrease productivity, economic, safety, and other environmental issues [0-4]. It was concluded that early faults detection is necessary to keep the cost in the industry by

keeping machine lifetime and spareparts. Therefore, the advanced maintenance systems move to another form of maintenance handling called predictive maintenance. So, it is based on condition monitoring to improve the productivity rate, production quality, and efficiency of manufacturing plants. The main concept of predictive maintenance is to achieve early detection of potential failures. When induction motors drive machines, predictive maintenance is used to find the root causes of these early failures (i.e., rotational unbalance, shaft misalignment, and bearing problems) and detect minor deflections before they occur. It is adequately

used to detect stator winding faults, broken rotors, and rotor air gap eccentricity. The benefit of early detection of a failing component is to avoid product failure due to overheating caused by faults and the energy use saved by switching it off.

More efforts were presented to detect and monitor the different faults initiated in rotary machines based on different condition monitoring methods. Independence-oriented variational mode decomposition method was proposed via correlation analysis to adaptively get the weak and compound fault feature of wheel set bearing[5]. Stochastic resonance was first investigated in a multi-stable system by computing its output spectral amplification, numerically analyzing its output frequency response, examining the effect of rescaling and damping factors on output responses, and finally presenting a method for initiating bearing fault diagnosis based on damped stochastic resonance with stable-state matching [6]. A multi-speed fault diagnostic approach was presented based on self-adaptive wavelet transform components produced from bearing vibration signals[7]. The presented approach can distinguish between signatures of four conditions of roller bearing, i.e., healthy bearing and three different types of defected bearings on the inner race, outer race, and roller separately. A bearing fault diagnosis technique was developed to increase the diagnosis accuracy[8]. Five features were selected as predictors in multi-class support vector machine (SVM) classification. The five selected features are entropy estimation error, mean, root mean squared (RMS) kurtosis, and histogram lower bound. A multi-fault diagnosis scheme for bearings was presented using hybrid features resulting from their acoustic emissions and a standard multi-class extension of the binary SVM [9]. Complete ensemble empirical mode decomposition (EEMD) was used with adaptive noise to detect rolling element bearings' faults [10]. The effect of sparse auto-encoder on the ordering performance of significantly compressed measurements of bearing vibration signals was displayed computationally [11].

One of the most used data identification methods for fault diagnosis is the machine learning and artificial neural network (ANN) algorithms. It can be observed that ANNs are used as classifiers based on the features extracted from collected data. Features characteristics have a significant influence on the results and signal processing techniques. Therefore, it is necessary to select the more

characteristic features in this scenario. A type of fault diagnosis algorithm was proposed based on manifold learning combined with a Wavelet Neural Network (WNN) [12]. The compressed sensing method was applied to get many compressed measurements of the primary bearing dataset. A Deep Neural Network (DNN) was performed for learning over complete sparse illustrations of these compressed datasets. An adaptive deep Conventional Neural Network (CNN) was proposed for roller bearing fault diagnosis[13]. Infrared thermography was used to monitor various conditions of roller bearings [14]. Two-dimensional Discrete Wavelet Transform (DWT) and Shannon entropy were implemented to decompose images for a certain decomposition level of approximated coefficients. The histograms of obtained coefficients were then employed as an input for the Genetic Algorithm (GA) and Artificial Neural Network (ANN) to achieve the most classification accuracy. Particle filtering and adaptive neuro-fuzzy inference system (ANFIS) approaches were used as fault prediction techniques [15]. The ANFIS learned the transition function of fault features, and then the practical filter algorithm predicted the remaining useful life of the gearbox.

In this research work, an improved monitoring solution based on vibration signatures is proposed to detect different faults in the rotating machines. The main objective is to extract unique features for each fault to avoid ambiguous diagnosis occurred in conventional fault diagnosis analysis. Section 2 introduces the experimental setup for the rotary machine test rig and definitions for applied mechanical faults. Then, the instrumentation and software are described in Section 3. Moreover, the signature analysis and machine learning method are discussed in section 4. The experimental results and analysis are presented in section 5. Finally, section 6 discusses the research conclusions.

## 2. Experimental Setup

The main objective of the test rig used in this research is to simulate common faults in rotary machines installed in many industries. Due to the nature of operating conditions and production requirements, the test rig operated nearly 12 hours to measure vibration signals resulted from healthy and different faulty cases at non stationary regimes (i.e. variable operating speed). The test rig was constructed from two shafts supported on

four bearings of UCP206 bearing type, as shown in Fig 1. The power is transmitted to the second shaft through pulleys and belts; each shaft carries one disc. A three-phase servo motor of APM-SE09MEK model type with a short shaft was used as a power source, and its speed was controlled by a servo drive of L7SA020A model type. The motor shaft was connected to a flexible coupling that assembled the motor shaft and the first shaft in the test rig.

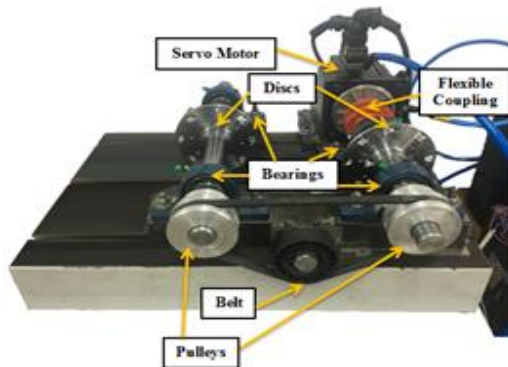


Fig 1: Test rig

Datasets of 104 cases were collected for healthy and different fault cases. The faults applied to the test rig are static unbalance, dynamic unbalance, pulley misalignment, belt damage, and combined faults as arranged in Table 1. The static unbalance was modeled as one weighted mass installed in the rotors of two shafts. The dynamic unbalance was modeled as two weighted masses; the angle between was slightly loosened to simulate the belt damage faults. Combined faults cases were simulated by testing the rig with two faults simultaneously (unbalance with pulley misalignment and unbalance with belt damage). Each fault case was tested at 500RPM (8.34Hz), 1000RPM (16.67Hz), 1500RPM (25Hz), and 2000RPM (33.33Hz) to study the ability to distinguish different faults in variable speed machines.

Table 1: Description for different fault cases

Symbol	Description	No of Cases			
		500 rpm	1000 rpm	1500 rpm	2000 rpm
C0	Healthy condition	1	1	1	1
C1	Static unbalance on one shaft	2	2	2	2
C2	Static unbalance on two shafts	9	9	9	9
C3	Dynamic unbalance	2	2	2	2
C4	Pulley misalignment	1	1	1	1
C5	Combined unbalance and pulley misalignment	5	5	5	5
C6	Belt damage	1	1	1	1
C7	Combined unbalance and belt damage	5	5	5	5

### 3. Instrumentation

A data acquisition system was used to trigger the data measured by sensors converted from analog to digital format at a specific sampling rate. B&K PULSE input module type 3050-A-060 was used as a data acquisition system in this analysis. It includes six high-precision input channels with an input range from DC to 51.2 kHz. A standard LAN cable was used for synchronous sampling between the module and system power. The module allows front panels to be interchanged freely, with various connectors for different transducers and applications. Electronic data sheet (TEDS) transducers were connected to the module, allowing intuitive front-end and analyzer setup based on TEDS information stored in the transducer such as family, serial number, sensitivity, and manufacturer. Two TEDS transducers were connected to the first two channels of the module, and each transducer was connected to the module by a Bayonet Neill–Concelman (BNC) cable of radiofrequency coaxial connector. The two transducers were used to measure the vibrational acceleration signals in the vertical and horizontal directions simultaneously on the same bearing.

Pulse Labshop software was setup, and vibration signals were collected through a frequency range from 0 to 400Hz, and time waveforms were sampled to 4096 samples to record 4sec and to satisfy Nyquist–Shannon sampling theorem ( $F_s =$

$2.56 \times F_{\max} = 1024 \text{ samples/sec}$ ). FFT spectra have 1600 lines of resolution, yielding a frequency resolution of 0.25Hz. On the other hand, the servo motor of APM-SE09MEK model type was connected to the APD-L7S servo drive, as shown in Fig 2 for complete control of the input and output parameters of the motor.

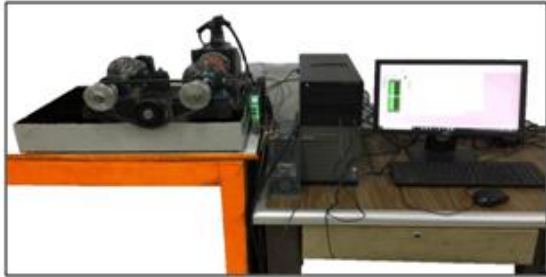


Fig 2: Configuration of data collection system

## 4. Analysis Methods

### 4.1 Vibration Signatures

The vibration analysis of the rotary machine is based on detecting mechanical faults associated with the operation and mounting of the machine. Almost of mechanical faults are detected in the low-frequency range ( $0 \sim 5f_0$ ), where  $f_0$  is the machine rotating frequency. For example, rotor unbalance and bent shaft can increase the amplitude at  $f_0$ , shaft misalignment increases the amplitude at  $f_0$ , and  $2f_0$ , external and internal looseness increases the amplitude  $f_0$ ,  $2f_0$ , ...,  $nf_0$ , where  $n$  is the harmonic number. These components can be defined by order,  $X$ , so,  $f_0$ ,  $2f_0$ , ...,  $nf_0$  is replaced by  $1X$ ,  $2X$ , ...,  $nX$ . Monitoring these components based on the signature of vibration analysis contributes to detecting these types of faults. In this research, the root means square (RMS) of time signal was estimated at two bearings for different fault cases and employed as an input vector to the ANN.

### 4.2 Machine Learning – Neural Networks

ANNs aim to duplicate the behavior of the human brain, which can generate specific illustrations such as objects or numbers. It is necessary to define the central processing unit called a neuron. The neuron in biological science is responsible for processing the information (in a signal form) received from the dendrites, which are the input way of signals, and then pass through the axon (the output path of the neuron). This process can be represented in ANN by a function called the transfer function. The transfer function determines

the output value of the neuron based on the overall values of its inputs. There are more functions employed as transfer functions, and the widely used is the sigmoid transfer function. The sigmoid output from each  $j^{\text{th}}$  neuron  $o[j]$  is represented from the following relation

$$o[j] = \frac{1}{\{1 + \exp(-i[j])\}} \quad (1)$$

Where  $i[j]$  is the sum of inputs to neuron  $j$ .

The architecture of ANN is composed of input, hidden, and output layers. The input layer is specified to receive the input, while the hidden layer is responsible for processing these data; the processed data are delivered by the output layer where the data can be viewed. The architecture of ANN can be represented by the scheme shown in Fig. 3. The network shown is composed of  $N$  input data inserted in the input layer, followed by the hidden layer with  $M$  neurons, and then  $L$  output data are achieved from the output layer.

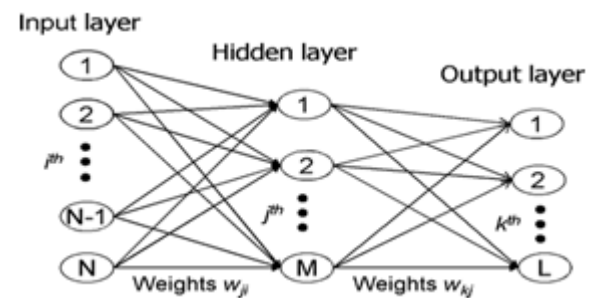


Fig 3: Schematic diagram of neural network

The back propagation neural network (BPNN) is one of the main methods constructed from multilayer networks. The algorithm of this network is based on the propagation-adaptation cycle since it computes the gradient of the loss function for a single weight by the chain rule. The network consists of an input pattern propagated from the first layer through hidden layer (s) ended at the output layer. Once the output is estimated, it is compared to the actual output, and the deviation (error) between two values is obtained through the following relation

$$\text{Error} = \text{Actual output} - \text{estimated output}$$

The error propagates from layer to layer from the entrance in the direction of exit till all neurons have received the error signal. After that, the data travel back from the output layer to the hidden layer (s) which modify their weights to allow the network to classify the training dataset correctly and decrease the error. The process is repeated until the desired

output is achieved. The importance of BPNN is represented in recognizing the characteristics of input data and minimizing the output error [16].

5. Results

5.1. Vibration dataset

FFT was computed for vibration signals, and the RMS at two bearings (No. 1 & 2) in the horizontal (Ht) direction was estimated and inserted in the ANN as the input vector. The vibration analysis was performed on the time waveform as displayed in the example shown in Fig 4. This figure presents the effect of unbalance fault on the vibration pattern and level since the unbalance increased the amplitudes at 2X, which is considered the dominant to increase the RMS of the time signal. The effect of different faults on changing the values of RMS levels is shown in Fig 5 and Table 2. However, there is an observed change in the levels of the selected vibration parameters; the simple frequency spectrum is not adequate for the diagnosis of some simulated faults without other aided tools[17], [18].

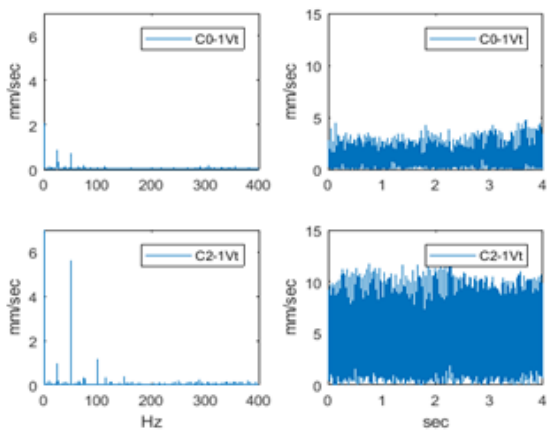


Fig 4: Frequency spectrum and time wave form for healthy and unbalance fault-1500rpm-Bearing No. (1)-vertical direction

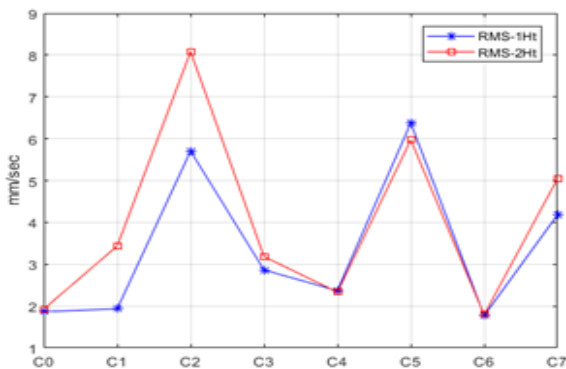


Fig 5: Variation of RMS for horizontal directions of two bearing-1500rpm

Table 2: RMS at bearing No. 1 & 2 in the horizontal direction-1500rpm

Case Type	C0	C1	C2	C3	C4	C5	C6	C7
RMS-1Ht (mm/s)	1.86	1.94	5.7	2.87	2.37	6.38	1.77	4.18
RMS-2Ht (mm/s)	1.93	3.44	8.08	3.18	2.33	5.98	1.79	5.05

5.2 Machine Learning - BPNN

A simple relation based on the size of training set may be useful for selecting the number neurons in the hidden layer as follow:

$$J = \log_2 P \tag{2}$$

where P is the number of training vectors used to train the ANN [19]. Another network learning improvement is based on repeated presentations for training samples which often produces good results and generalizations in some applications [19]. In this analysis, each sample in the training set was used three times in the training stage. Four-layer BPNN and 20 neurons in each hidden layer were built, as shown in Fig 6, using log-sigmoid and tan-sigmoid transfer functions in the hidden and output layer, respectively. The training performance and accuracy are displayed in Fig 7 and Fig 8. It was found that the training, test, and validation performance achieve the same pattern and the best validation was recorded at 0.3304 mean squared error (MSE). The training accuracy could be estimated by using the following formula

$$\text{Accuracy} = \frac{\sum_{i=1}^{N_c} w}{N_c} \times 100 (\%) \tag{3}$$

where  $N_c$  is the number of simulated cases for the same type of fault, w is the recorded weight for each case since if the network output equals the simulated case,  $w = 1$ , else,  $w = 0$ . It was found that the network can identify combined pulley misalignment with unbalance, static unbalance on two shafts, dynamic unbalance, and combined belt damage with unbalance faults with identification accuracy of 95, 92, 88, and 80%, respectively. Static unbalance, pulley misalignment, and belt damage faults come in the second level of accuracy since they have the same accuracy of 75%. The training accuracy for all cases is arranged in Table 3.

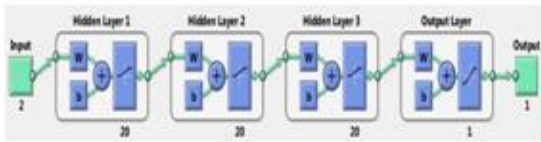


Fig 6: Feed forward BPNN architecture

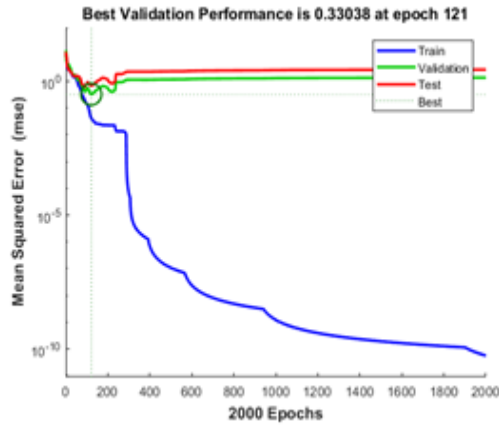


Fig 7: Neural network validation performance

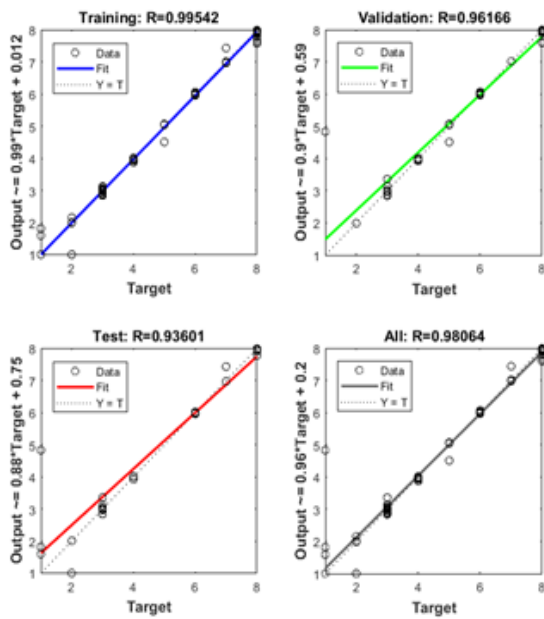


Fig 8: Neural network regression

Table 3: Identification accuracy for healthy and faulty cases

Case Type	C0	C1	C2	C3	C4	C5	C6	C7
No of Cases (N)	12	24	108	24	12	60	12	60
Accuracy %	60	75	92	88	75	95	75	80

**6. Conclusions**

Fault detection of rotating machine based on vibration measurement and machine learning algorithm was presented in the research. Vibration time signals were analyzed and their RMS at different bearings were estimated for training the

BPNN. It was found that the test and validation performance achieve the same pattern and the best validation was recorded at 0.33038 mean squared error (MSE). This training accuracy can identify combined pulley misalignment with unbalance, static unbalance on two shafts, dynamic unbalance, and combined belt damage with unbalance faults with identification accuracy of 95, 92, 88, and 80%, respectively. Static unbalance, pulley misalignment, and belt damage faults come in the second level of accuracy since they have the same accuracy of 75%. Furthermore, this network has a superior improvement in detecting combined faults in addition to other single variable faults. More features, which have significant variations with different cases, have to be selected as input parameters to the ANN to improve the training and identification accuracy for healthy and different fault cases.

**References**

- [1] N. Verma, T. Subramanian, Cost benefit analysis of intelligent condition based maintenance of rotating machinery, 7th IEEE Conference on Industrial Electronics and Applications (ICIEA) (2012), pp. 1390-1394.
- [2] Z. Zhang, Data mining approaches for intelligent condition-based maintenance, a framework of intelligent fault diagnosis and prognosis System (IFDPS) (2014).
- [3] S. Shao, W. Sun, P. Wang, R. Gao, R. Yan, Learning features from vibration signals for induction motor fault diagnosis, International Symposium on Flexible Automation (ISFA) IEEE (2016), pp. 71-76.
- [4] O. Abdeljaber, O. Avci, S. Kiranyaz, M. Gabbouj, D. Inman, Real-time vibration-based structural damage detection using one-dimensional convolutional neural networks, Journal of Sound and Vibration (2017), vol. 388, pp. 154-170.
- [5] Z. Li, J. Chen, Y. Zi, J. Pan, Independence-oriented VMD to identify fault feature for wheel set bearing fault diagnosis of high speed locomotive, Mechanical Systems and Signal Processing (2017), vol. 85, pp. 512-529.
- [6] Y. Lei, Z. Qiao, X. Xu, J. Lin, S. Niu, An underdamped stochastic resonance method with stable-state matching for incipient fault diagnosis of rolling element bearings, Mechanical Systems and Signal Processing (2017), vol. 94, pp. 148-164.
- [7] Z. Huo, Y. Zhang, P. Francq, L. Shu, J. Huang, Incipient fault diagnosis of roller bearing using optimized wavelet transform based multi-speed vibration signatures, IEEE Access 5 (2017) pp. 19442-19456.

- [8] D. Susilo, A. Widodo, T. Prahasto, M. Nizam, Fault diagnosis of roller bearing using parameter evaluation technique and multi-class support vector machine, AIP Conference Proceedings (2017), vol. 1788, p. 030081.
- [9] M. Islam, J. Kim, S. Khan, J. Kim, Reliable bearing fault diagnosis using Bayesian inference-based multi-class support vector machines, The Journal of the Acoustical Society of America (2017), vol. 141, pp. 89-95.
- [10] Y. Lei, Z. Liu, J. Ouazri, J. Lin, A fault diagnosis method of rolling element bearings based on CEEMDAN, Journal of Mechanical Engineering Science (2017), vol. 231, pp. 1804-1815.
- [11] H. Ahmed, M. Wong, A. Nandi, Intelligent condition monitoring method for bearing faults from highly compressed measurements using sparse over-complete features, Mechanical Systems and Signal Processing (2018), vol. 99, pp. 459-477.
- [12] L. Wu, B. Yao, Z. Peng, Y. Guan, Fault diagnosis of roller bearings based on a wavelet neural network and manifold learning, Applied Sciences (2017), vol. 7, p. 158.
- [13] F. Wang, H. Jiang, H. Shao, W. Duan, S. Wu, An adaptive deep convolutional neural network for rolling bearing fault diagnosis, Measurement Science and Technology (2017), vol. 28, p. 095005
- [14] Z. Huo, Y. Zhang, R. Sath, L. Shu, Self-adaptive fault diagnosis of roller bearings using infrared thermal images, 43rd Annual Conference of the IEEE Industrial Electronics Society (2017), pp. 6113-6118.
- [15] F. Cheng, L. Qu, W. Qiao, Fault prognosis and remaining useful life prediction of wind turbine gearboxes using current signal analysis, IEEE Transactions on Sustainable Energy (2017), vol. 9, pp. 157-167.
- [16] J. Zafra, R. Moreno, R. Hernández, Comparison between Backpropagation and CNN for the Recognition of Traffic Signs, International Journal of Applied Engineering Research (2017), vol. 12, pp. 6814-6820.
- [17] J. Sinou, Experimental response and vibrational characteristics of a slotted rotor, Communications in Nonlinear Science and Numerical Simulation (2009), vol. 14, pp. 3179-3194.
- [18] J. Sinha, Health monitoring techniques for rotating machinery, PhD University of Wales Swansea (2002).
- [19] Z. Jacek, Introduction to Artificial Neural Systems [M], St. Paul: West Publishing Company (1992), pp. 57-60.